Available online at www.sciencedirect.com
ScienceDirect
Journal of the European Ceramic Society 29 (2009) 3395–3400
www.elsevier.com/locate/jeurceramsoc

Static and dynamic mechanical properties of boron carbide processed by spark plasma sintering

S. Hayun [a], V. Paris [b], M.P. Dariel [a], N. Frage [a,*], E. Zaretzky [b]

[a] *Department of Materials Engineering, Ben-Gurion University of the Negev, P.O. Box 653, Beer-Sheva 84105, Israel*
[b] *Department of Mechanical Engineering, Ben-Gurion University of the Negev, P.O. Box 653, Beer-Sheva 84105, Israel*

Received 27 April 2009; accepted 13 July 2009
Available online 14 August 2009

Abstract

Spark plasma sintering (SPS) has become a popular technique for the densification of covalent ceramics. The present investigation is focused on the static mechanical properties and dynamic compressive behavior of SPS consolidated boron carbide powder without any sintering additives. Fully dense boron carbide bodies were obtained by a short high temperature SPS treatment. The mechanical properties of the SPS-processed material, namely hardness (32 GPa), Young modulus (470 GPa), fracture toughness K_C (3.9–4.9 MPa $m^{0.5}$), flexural strength (430 MPa) and Hugoniot elastic limit (17–19 GPa) are close or even better than those of hot-pressed boron carbide.

Keywords: Boron carbide; Spark plasma sintering (SPS); Mechanical properties; Dynamic properties; Hugoniot elastic limit

1. Introduction

The outstanding properties of boron carbide make it a valuable potential material for a variety of applications.[1–7] The major drawback hindering the realization of boron carbide potential is a very high temperature required for its sintering.[8] Over the past years the, spark plasma sintering (SPS) or Field Assisted Sintering Technology (FAST),[9–12] as it is commonly called, has gained a great popularity for the processing of a wide variety of materials. Dipanker et al.[10] applied this technology to submicron, 800 nm, boron carbide powder, and reached 99.2% relative density. Recently,[13] we reported the SPS conditions that allow fabricating fully dense boron carbide specimens in the absence of any sintering additives. The mechanical properties of B_4C fabricated by traditional (hot-press and pressure-less sintering) technologies has been studied extensively in the course of the past few decades. The static mechanical properties were reviewed by Thévenot.[1] The dynamic response and, in particular, the Hugoniot elastic limit (HEL) has been studied by planar impact technique.[14–20] It was established that the mechanical properties of boron carbide, namely, its elastic moduli, flexural strength, hardness, and HEL decline with increasing the material porosity and grain size. Such information concerning the SPS-processed boron carbide is absent. The present communication should fill this gap, presenting the results of an experimental investigation of the static mechanical behavior of the SPS-consolidated boron carbide as a function of its porosity, as well as the planar impact response of fully dense boron carbide obtained by using the SPS technique.

2. Materials

Boron carbide samples were sintered by SPS without any sintering additive. Boron carbide powder (grade HS supplied by H.C. Starck Company, Germany) was placed into graphite dies with 20 or 30 mm inner and 40 or 50 mm outer diameters, respectively. The dies were wrapped with a 20-mm thick graphite wool for thermal insulation (Fig. 1). After placing the die in the SPS apparatus (type HP D5/1, FCT System, Rauenstein, Germany), equipped with a 50-kN uniaxial press the sintering procedure was conducted in a vacuum of 10^{-2} Torr under 32 MPa pressure. By varying the sintering temperature between 1900 and 2200 °C, it became possible to fabricate boron carbide specimens with relative densities ranging from 0.8 to 1.

The sintering behavior and the microstructural features of the obtained specimens were discussed elsewhere.[13] In the present

* Corresponding author. Tel.: +972 8 6461468; fax: +972 8 6489441.
E-mail address: nfrage@bgu.ac.il (N. Frage).

0955-2219/$ – see front matter © 2009 Elsevier Ltd. All rights reserved.
doi:10.1016/j.jeurceramsoc.2009.07.007

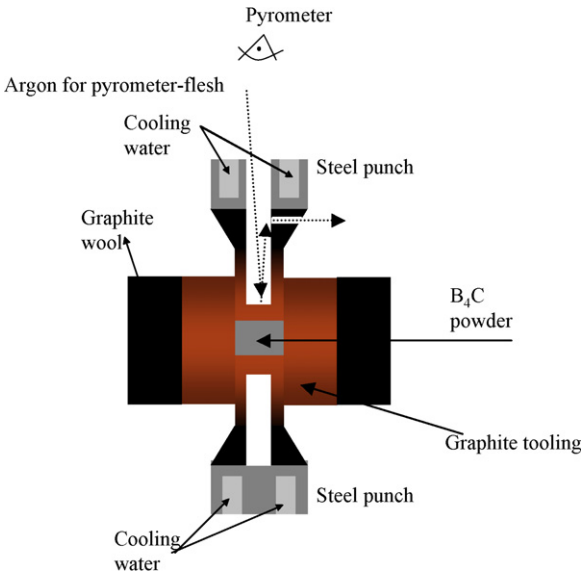

Fig. 1. Schematic set-up of SPS tools.

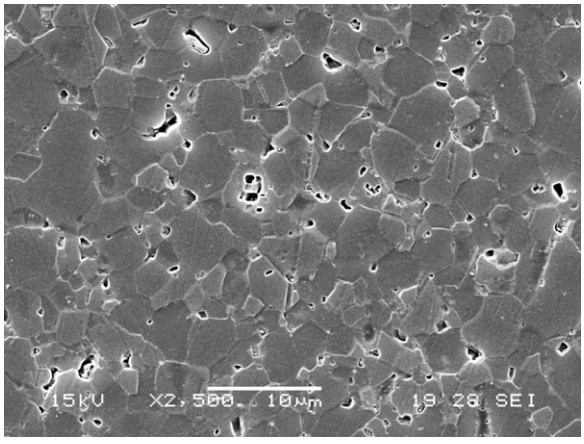

Fig. 2. SEM micrographs of SPS-processed nearly fully dense boron carbide.

study the static mechanical properties (Young modulus and flexural strength) of the specimens with different relative densities were measured. In the evaluation of the dynamic behavior of the SPS-consolidated material only nearly fully dense specimens were employed. The microstructure of the fully dense boron carbide (0.8–1.0 vol.% porosity measured by water displacement method) is presented in Fig. 2. It consists of the equiaxed fine grains of 4.05 ± 1.62 μm average size and some apparent residual porosity slightly higher than 1.0 vol.%. We believe that the micrograph-apparent porosity excess originates from the sample preparation procedure (polishing and etching) and is caused by the pull-out of the fine particles.

3. Experimental

3.1. Static mechanical properties

The hardness of the SPS-processed boron carbide samples was determined by Buehler-Micromet 2100 microhardness tester with a Vickers indenter under 5 and 20 N loads. The flexural strength was determined by the three-point bending test on 3 mm × 4 mm × 20 mm bars in an LRX Plus LLOYD instrument (Lloyd Instruments, Fareham Hants, U.K.). The velocities of the longitudinal C_l and shear C_S acoustic waves were measured by a pulse-echo technique using a 5 MHz probe. The elastic moduli were derived from the ultrasonic velocity data and the density values of the specimens measured by the Archimedes method.

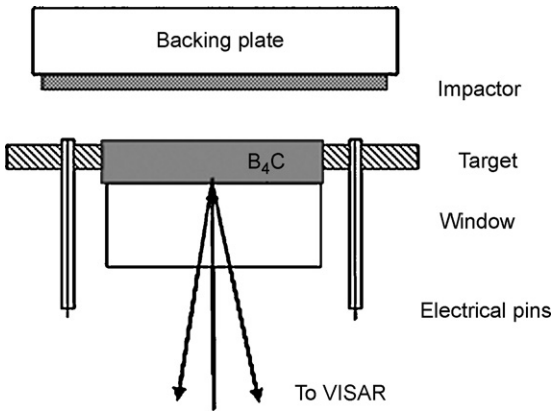

Fig. 3. Plate impact test set-up with VISAR diagnostics.

3.2. Dynamic behavior

To characterize the response of the material to dynamic (impact) compressive loading a series of planar impact experiments was carried out on a single stage 25-mm diameter, 6 m long gas gun. The gun is capable of accelerating the PMMA projectile equipped with an impactor of 1–2 mm thickness to a velocity of about 1.2 km/s. The impactors were tungsten (1.1–1.2 mm thickness) or copper (0.5 and 1 mm thickness) discs of 24.5 mm diameter. A schematic of the impact experiments is shown in Fig. 3. For the impact testing the boron carbide specimens were polished to ensure a 5-μm parallelism of the specimen surfaces. The reflectivity of the rear (unimpacted) surface of the specimens was enhanced by either a layer of 15-μm aluminum foil (three tests) or a 1-μm layer of vapor-deposited gold. In order to prevent the loss of reflectivity caused by the arrival of the shock at the sample surface, 6-mm PMMA windows were glued on the coated rear surface of the specimen (Fig. 3). The velocity of the specimen-window interface was continuously monitored by VISAR.[21] Four electrically charged pins were used for measuring the impact velocity and for the control of the impactor-specimen misalignment (the latter did not exceed 0.5 mrad in all the experiments).

4. Results and discussion

4.1. Static mechanical properties

The Young's modulus and the flexural strength of the sintered specimens as the functions of the measured relative density are shown in Fig. 4. Fully dense material displays a slightly higher Young's modulus value (470 ± 7 GPa) than commercial hot-pressed (HP) boron carbide (460 GPa). The value of the flexural strength (430 ± 21 MPa) is similar to that of HP boron carbide.[1]

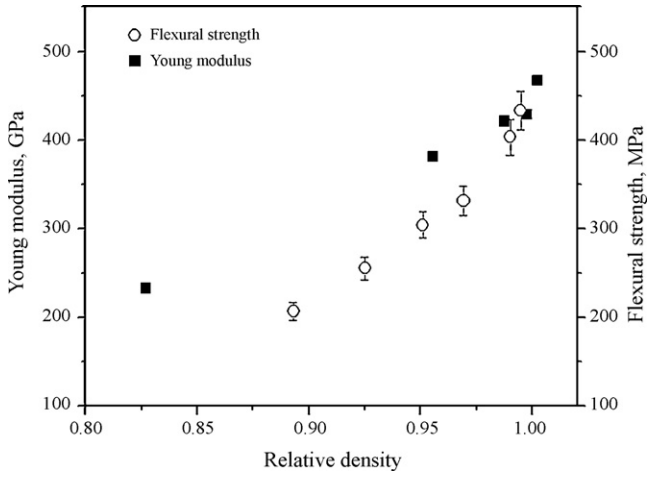

Fig. 4. The Young's modulus and the flexural strength as a function of the measured relative density.

The Vickers hardness of fully dense specimens was determined as an average after 10 indentations on three specimen (20 N load) and was found equal to $H_V = 32 \pm 2$ GPa. This value together with the measured lengths of the cracks generated at the corners of the imprints was used for evaluation of the ceramic fracture toughness (K_C).[22–24] The crack patterns produced in the indented sample by the Vickers indenter may be of two distinct types. One is the median crack system, which consists of two half-penny-shaped cracks,[25] and the other is the Palmqvist crack system, which consists of four cracks of semi-elliptical shape.[26] Each type of the crack systems results in the different expressions for the K_C calculation. In order to identify the type of the crack an additional, post-indentation, polishing was performed. The optical images of the indentation vicinity just after the indentation and after the subsequent polishing, Fig. 5, suggest that the cracks appearing under the indentation of the SPS-processed boron carbide are Palmqvist cracks.

The equations suggested in refs. 23, 24 for estimating the K_C values in the case of the Palmqvist crack are presented in Table 1 together with the corresponding K_C values. The K_C values are between 3.9 and 4.9 MPa m$^{0.5}$. Lee and Speyer[27] and Dipankar et al.[10] have also used the length of the cracks generated at the corners of the imprints in order to evaluate the fracture toughness of the boron carbide specimens produced by pressureless sintering and Plasma Pressure Compaction ($P^2C^®$) technique, respectively. However the authors determined the nature of the crack system by fitting the equation of type $y = bx^n$ to the relationships, $c = AP^{2/3}$ in the case of half-penny cracks and $l = BP$ in the case of Palmqvist cracks and concluded that the half-penny crack system exists without any additional microstructural characterization. The K_C values that they reported ranged from 2.8 to 3.1 MPa m$^{0.5}$, and from 3.2 to 3.6 MPa m$^{0.5}$ for the specimens obtained by pressureless sintering and the $P^2C^®$ technique, respectively.

4.2. Dynamic properties

Parameters of the plate impact experiments performed with five boron carbide specimens are given in Table 2 together with the HEL values obtained in the experiments. The B_4C/PMMA interface velocity profiles $w_{if}(t)$ recorded in the experiments with the gold and the aluminum reflectors are shown in Fig. 6a and b, respectively. The spike-like features at the upper part of the elastic precursor front (Fig. 6b) are due to the finite (14–15 μm) thickness of the aluminum foil reflector. For the velocity profiles obtained with the sputtered gold reflector of submicron thickness the spike-like features are absent (Fig. 6a). Thus, for the velocity profiles of Fig. 6b the immediate post-spike interface velocity

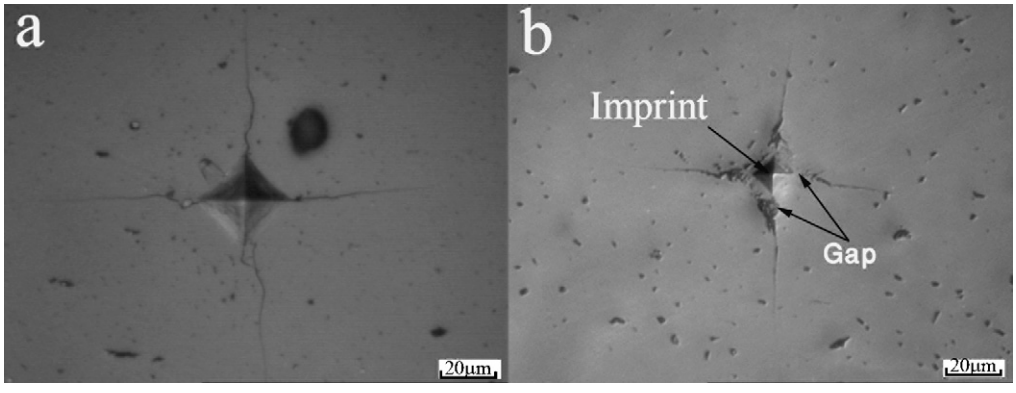

Fig. 5. Optical images of a Vickers imprint just after the indentation (a), and after the subsequent polishing (b). The right image shows a gap between the crack and the imprint indicating the Palmqvist crack.

Table 1
Calculated K_C values from different equations for Palmqvist crack system.

Equation	K_C (MPa m$^{0.5}$)		Ref.
	$P = 5$ N	$P = 20$ N	
$K_C = 0.0264(H_V a)(E/H_V)^{0.4}(l^{-0.5})$	4.31 ± 0.20	4.93 ± 0.30	[23]
$K_C = 0.0937(H_V P/4l)^{0.5}$	3.90 ± 0.29	4.36 ± 0.32	[24]

Table 2
Summary of some B_4C properties and results of plate impact tests.

Test	Impact velocity (km/s)	Impactor material	Impactor/target thickness (mm)	Density (g/cm^3)	C_l (km/s)	C_b (km/s)	Peak stress[c] (GPa)	σ_{HEL} (GPa)	Y_D, GPa (Griffith)	Y_D, GPa (von Mises)
BCA[a]	1.163	Cu	0.496/3.277	2.495	13.54	9.26	21.5	18.7	9.9	14.9
BCB[a]	1.131	Cu	1.005/4.276	2.504	13.69	9.38	21.5	18.7	9.8	14.9
BCC[a]	1.061	W	1.182/4.285	2.506	13.62	9.31	23.0	18.2	9.7	14.5
BCF[b]	0.926	W	1.176/5.240	2.517	13.94	9.55	21.5	17.1	9.0	13.6
BCI[b]	1.030	W	1.080/5.242	2.508	13.87	9.51	22.5	19.0	9.9	15.1

[a] The shots performed with aluminum foil at the sample- window interface.
[b] The shots performed with vapor deposited gold layer at the sample- window interface.
[c] The stress corresponds to a part of the sample adjacent to impact surface.

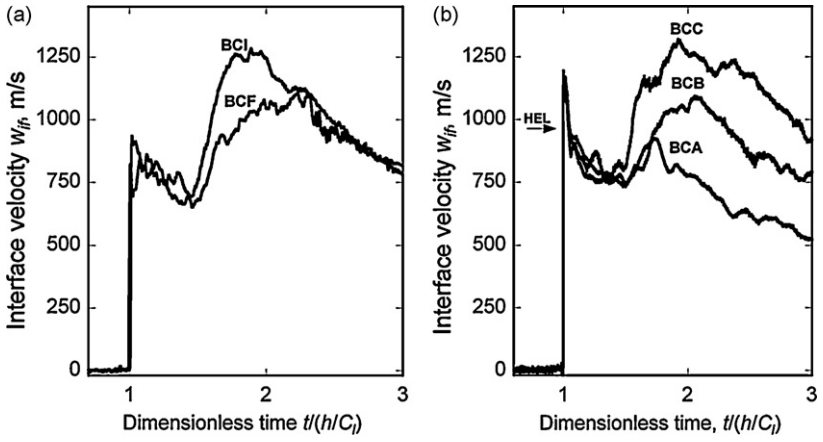

Fig. 6. VISAR-collected waveforms of the B_4C/PMMA interface velocity recorded in the plate impact tests listed in Table 2. In order to eliminate the difference in the thickness of the samples, the time is normalized over the period required for the passage of the elastic precursor wave through the sample.

values w_{if}^{HEL}, were used for determination of the boron carbide HEL. The stress values at HEL were calculated according to the formula:

$$\sigma_{HEL} = \frac{1}{2} w_{if}^{HEL} \cdot [(\rho C_l)_{Cer} + (\rho D)_{PMMA}] \quad (1)$$

where $(\rho_0 C_l)_{Cer}$ is the shock elastic impedance of the ceramic and $(\rho_0 D)_{PMMA}$ is the shock impedance of the PMMA window. The latter was derived from the PMMA Hugoniot data.[28] The calculated values of σ_{HEL} are in the 17–19 GPa range (Table 2). The uncertainty of the HEL determination is ±5%. It should be noted that the σ_{HEL} value evaluated from the BCF profile is slightly lower than others even though this sample exhibit both higher density and the higher elastic wave speed.

Comparison between the present data and the HELs of HP boron carbide as reported in the literature,[17,18,20,29] as a function of the grain size is presented in Fig. 7. The HEL data reported by refs. 17, 20 as well as the results of the present study, are associated with less than 1 vol.% porosity. The HEL values reported by Brar et al.[18] and Zaretsky et al.[29] were obtained with samples having 1–15 vol.% and 1–6 vol.% porosity, respectively. In Fig. 7 only the maximum and minimum HEL values, corresponded to the porous and near fully dense samples, are presented. It is apparent that within experimental inaccuracy the presently studied samples display HEL values close to those of the hot-pressed boron carbide with similar porosity and grain size.[17,18,20,29]

All the velocity profiles display a jagged velocity decline from 900–930 to 700–750 m/s just immediately behind the elastic precursor front. The duration of the decline in the dimensionless time units is approximately 0.5. The velocity decline is associated with a post-HEL drop of the compressive stress caused, possibly, by the failure of the sample material under

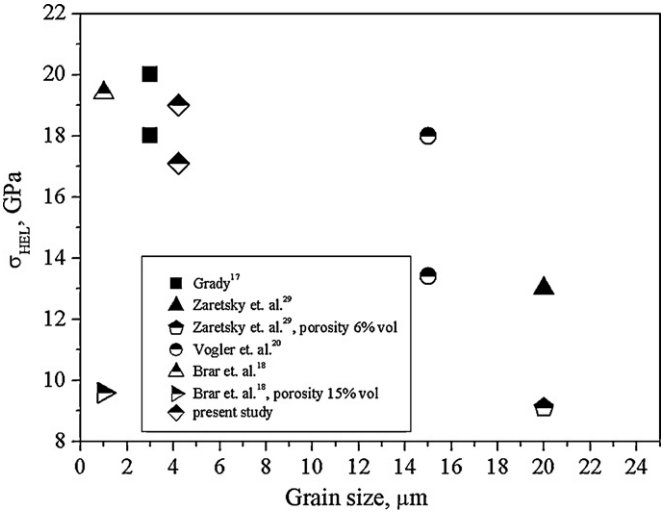

Fig. 7. Minimum and maximum values of stress at HEL as a function of the grain size of the boron carbide samples. Points with porosity higher then 1% indicated in the figure.

compression. This drop of the interface velocity to 700–750 m/s is followed by the velocity rise associated with arrival of the bulk compressive wave. The first indication of the bulk compressive wave on the profiles corresponds to wave velocities ranging from 8.3 to 9.5 km/s depending on the peak stress in the test. A similar post-HEL behavior was observed in the planar impact experiments with hot-pressed B_4C samples and with the same grain size.[17]

The commonly used correlation $H_V \approx 3Y_c$[30–32] between the compressive strength Y_c and Vickers hardness H_V was applied in order to evaluate the mode of inelastic dynamic behavior of the SPS-processed boron carbide.

For the dynamic threshold stress Y_D corresponding to the onset of the brittle material fracture in compression, the expression derived by Rozenberg from Griffith's brittle failure criterion[33] was applied

$$Y_D^{\mathrm{br}} = \frac{(1-2\nu)^2}{1-\nu}\sigma_{\mathrm{HEL}}, \tag{2}$$

where ν is the Poisson's ratio. The data of Table 2 yield the values of Y_D^{br} ranging from 9 to 10 GPa. Using the experimentally determined Vickers hardness $H_V = 32 \pm 2$ GPa and Eq. (2) the H_V/Y_D^{br} value is equal to 3.25 ± 0.25 was obtained. At the same time, using for Y_D the expression $Y_D^{\mathrm{duct}} = (1 - 2\nu/(1-\nu))\sigma_{\mathrm{HEL}}$, based on von Mises criterion of a ductile inelastic material behavior, the value of H_V/Y_D^{duct} is equal to 2.25 ± 0.25. Thus, the first value (3.25 ± 0.25) is in a reasonable agreement with the commonly used value for brittle solids proposed by Rozenberg[34] and it may be concluded that the inelastic response of the SPS-processed B_4C ceramic is that of a brittle material.

5. Summary

Boron carbide sintered using the SPS technique has a fine grain structure and its density is close to the theoretical density. It displays higher mechanical properties, static and dynamic, and the processing time is much shorter than that required for the routine hot-pressed material. It should be noted that the temperature and the applied pressure are close to those required for the hot-pressing. The nature of the crack system generated by the micro hardness indentations in the SPS-processed boron carbide corresponds to that of the Palmqvist crack system. The fracture toughness values (3.9–4.9 MPa $m^{1/2}$) are higher then those reported for half-penny cracks (2.8–3.6 MPa $m^{1/2}$). The impact response of the dense SPS B_4C is characterized by high (17–19 GPa) HEL values, equal or even higher than those of the hot-pressed boron carbide with similar grain size and porosity. The failure threshold (Y_D) values, estimated based on the HEL values, clearly show that the inelastic response of the SPS-processed B_4C is similar to that of the hot-pressed boron carbide of identical microstructure and indicate brittle behavior of the material. To summarize, the SPS-processing of boron carbide ceramics allows faster and cheaper fabrication of the final product without any loss of mechanical performance.

Acknowledgment

This work was supported by the Israel Ministry of Science grant 3-3429.

References

1. Thévenot, F., Boron carbide—a comprehensive review. *J. Eur. Ceram. Soc.*, 1990, **6**, 205–225.
2. Kim, W. H., Koh, Y. H. and Kim, H. E., Densification and mechanical properties of B_4C with Al_2O_3 as a sintering aid. *J. Am. Ceram. Soc.*, 2000, **83**, 2863–2865.
3. Skorokhod, V. J., Vlajic, M. D. and Krstic, V. D., Mechanical properties of pressureless sintered boron carbide containing TiB_2 phase. *J. Mater. Sci. Lett.*, 1996, **15**, 1337–1339.
4. Schwetz, K. A. and Grellner, W., The influence of carbon on the microstructure and mechanical properties of sintered boron carbide. *J. Less-Common Met.*, 1981, **82**, 37–47.
5. Sigl, L. S., Processing and mechanical properties of boron carbide sintered with TiC. *J. Eur. Ceram. Soc.*, 1998, **18**, 1521–1529.
6. Levin, L., Frage, N. and Dariel, M. P., Effect of Ti and TiO_2 additions on the pressureless sintering of B4C. *Metall. Mater. Trans. A*, 1999, **30**, 3021–3210.
7. Seifert, H. J. and Aldinger, F., Phase equilibria in the Si–B–C–N system. *Struct. Bond. (Berlin, Ger.)*, 2002, **101**, 1–58.
8. Lee, H. and Speyer, R. F., Pressureless sintering of boron carbide. *J. Am. Ceram. Soc.*, 2003, **86**, 1468–1473.
9. Klotz, B. R., Cho, K. R. and Dowding, R. J., Sintering aids in the consolidation of boron carbide (B_4C) by the plasma pressure compaction (P^2C) method. *Mater. Manuf. Process*, 2004, **19**, 631–639.
10. Dipankar, G., Ghatu, S., Tirumalai, S. S., Ramachandran, R. and Xin-Lin, G., Dynamic indentation response of fine-grained boron carbide. *J. Am. Ceram. Soc.*, 2007, **90**, 1850–1857.
11. Anselmi-Tamburini, U., Munir, A. Z., Kodera, Y., Imai, T. and Ohyanagi, M., Influence of synthesis temperature on the defect structure of boron carbide: experimental and modeling studies. *J. Am. Ceram. Soc.*, 2005, **88**, 1382–1387.
12. Frage, N., Hayun, S., Kalabukhov, S. and Dariel, M. P., The effect of Fe addition on the densification of B4C powder by spark plasma sintering. *Powder Metall. Met. Ceram.*, 2007, **46**, 533–538.
13. Hayun, S., Kalabukhov, S., Ezersky, V., Dariel, M. P. and Frage, N. Microstructural characterization of Spark Plasma Sintered Boron Carbide Ceramics. *Ceram. Int.*, in press.
14. Kipp, M. E. and Grady, D. E., Shock compression and release in high-strength ceramics. In *Shock Compression of Condensed Matter 1989*, ed. S. Schmidt C., J. N. Johnson, W. L. Davison and W. North-Holland. Amsterdam, 1990, pp. 377–380.
15. Winkler, W. and Stilp, A. J., Spallation behavior of TiB_2, SiC, and B_4C under planar impact tensile stress. In *Shock Compression of Condensed Matter*, ed. S. C. Schmidt *et al.* North-Holland, New York, 1992, pp. 475–478.
16. Grady, D. E., Shock wave properties of high strength ceramics. In *Shock Compression of Condensed Matter*, ed. S. C. Schmidt *et al.* North-Holland, New York, 1992, pp. 455–458.
17. Grady, D. E., Shock-wave strength properties of boron carbide and silicone carbide. *J. Phys. IV*, 1994, **C8**, 385–391.
18. Brar, N. S., Rosenberg, Z. and Bless, S. J., Applying Steinberg's model to Hugoniot elastic limit of porous boron carbide specimens. *J. Appl. Phys.*, 1991, **69**, 7890–7891.
19. Dandekar, D. P., *Shock Response of Boron Carbide*. U.S. Army Materials Technology Laboratory, Aberdeen Proving Ground, MD, 2001 (RL-TR-2456).
20. Vogler, T. J., Reinhart, W. D. and Chhabildas, L. C., Dynamic behavior of boron carbide. *J. Appl. Phys.*, 2004, **95**, 4173–4183.
21. Barker, L. M. and Hollenbach, R. E., Laser interferometer for measuring high velocities of any reflecting surface. *J. Appl. Phys.*, 1972, **43**, 4669.

22. Ponton, C. B. and Rawlings, R. D., Vickers indentation fracture toughness test, part 1, review of literature and formulation of standardized indentation toughness equations. *Mater. Sci. Tech.*, 1989, **5**, 865–872.
23. Niihara, K., A fracture mechanics analysis of indentation-induced Palmqvist cracks in ceramics. *J. Mater. Sci. Lett.*, 1983, **2**, 221–223.
24. Shetty, D. K., Wright, I. G., Mincer, P. N. and Clauer, A. H., Indentation fracture of WC–Co cermets. *J. Mater. Sci.*, 1985, **20**, 1873–1882.
25. Evans, A. G. and Charles, E. A., Fracture toughness determinations by indentation. *J. Am. Ceram. Soc.*, 1976, **59**, 371–372.
26. Palmqvist, S., Occurrence of crack formation during Vicker indentation as a measure of the toughness of hard metals. *Arch. Eisenhuttenwes*, 1962, **33**, 629–633.
27. Lee, H. and Speyer, R. F., Hardness and fracture toughness of pressureless-sintered boron carbide (B_4C). *J. Am. Ceram. Soc.*, 2002, **85**, 1291–1293.
28. Marsh, S. P., *LASL Shock Hugoniot Data*. University of California Press, Berkeley, 1980.
29. Zaretsky, E. B., Paris, V. E., Kanel, G. I. and Savinykh, A. S., Evidence of ductile (alumina) and brittle (boron carbide) response of ceramics under shock wave loading. *Ceram. Trans.*, 2003, **151**, 105–115.
30. Gilman, J. J., Relationship between impact yield stress and indentation hardness. *J. Appl. Phys.*, 1975, **46**, 1435–1436.
31. Lankford, J., The compressive strength of strong ceramics: micro-plasticity versus micro-fracture. *J. Hard Mater.*, 1991, **2**, 55–77.
32. Dunlay, W. A., Tracy, C. A. and Perrone, P. J., *A Proposed Uniaxial Compression Test For High Strength Ceramics*. U.S. Army Materials Technology Laboratory, 1989 (MTL TR 89-89).
33. Rozenberg, Z., On the relation between the Hugoniot elastic limit and the yield strength of brittle materials. *J. Appl. Phys.*, 1993, **74**, 752–754.
34. Rozenberg, Z., On the correlation between dynamic compressive strengths of strong ceramics and their indentation hardness. In *Proceedings of the Conference of the American Physical Society Topical Group on Shock Compression of Condensed Matter*, ed. S. C. Schmidt and W. C. Tao. AIP, New York, 1996, pp. 543–546.